IJMSO

International Journal of Mathematical Sciences and Optimization: Theory and Applications
11(4), 2025, Pages 69 - 82
https://doi.org/10.5281/zenodo.18987204

Impact of Suction/Injection on MHD Natural Convection Couette Flow in a Vertical Porous Channel in the Presence of Nonlinear Boussinesq Approximation

M. K. Tafida [1*], A. Y. Abdullahi [1], M. Yahuza [1]

1. Department of Mathematics, Federal University of Education, Zaria, Nigeria.
* Corresponding author: mktafida.555@gmail.com, myahuza85@gmail.com, yuhaishmaya@gmail.com

Article Info
Received: 13 June 2025 Revised: 02 October 2025
Accepted: 11 November 2025 Available online: 30 January 2026

Abstract

This study analytically investigates buoyancy driven magnetohydrodynamic (MHD) natural convection Couette flow in a vertical channel, focusing on the effects of the nonlinear Boussinesq approximation, suction/injection and magnetic fields. The nonlinear Boussinesq term captures significant thermal variations beyond linear models, suction/injection modifies boundary-layer thickness and convective transport, and the magnetic field introduces Lorentz-force damping in electrically conducting flows. The governing momentum and energy equations are solved using the Homotopy Perturbation Method (HPM), and the influence of various parameters on velocity and temperature distributions is examined. Results indicate that the nonlinear Boussinesq parameter enhances fluid motion near the moving plate while suppressing it near the stationary plate. Increased Hartmann numbers uniformly dampen velocity due to stronger Lorentz forces, whereas suction/injection modulates flow development by adjusting the boundary layer. The findings highlight the interplay of buoyancy, magnetic suppression and boundary layer control, providing insights for optimizing flow stability and heat transfer in advanced thermal fluid systems.

Keywords: Couette flow, Magnetohydrodynamic, Natural convection, Nonlinear Boussinesq Approximation, Vertical channel.
MSC2010: 47H10, 47J25.

1 Introduction

Natural convection Couette flow refers to a heat transfer mechanism in which fluid motion is driven by density variations resulting from temperature differences. This phenomenon has found widespread application over the years, particularly as a cooling method in nuclear reactors, electronic devices, and microchips. Suction and injection significantly influence boundary-layer behavior in porous channels, with suction enhancing flow stability by suppressing boundary-layer growth

IJMSO

International Journal of Mathematical Sciences and Optimization: Theory and Applications
11(4), 2025, Pages 69 - 82
https://doi.org/10.5281/zenodo.18987204

and injection promoting mixing but potentially destabilizing the flow. These mechanisms are relevant to engineering applications such as aerospace boundary-layer control, turbine blade cooling, and porous media filtration. Similarly, magnetohydrodynamics (MHD) governs the interaction between magnetic fields and electrically conducting fluids, where the resulting Lorentz force dampens velocity, suppresses turbulence, and stabilizes the flow. Practical applications of MHD include electromagnetic casting, liquid metal cooling in nuclear reactors, plasma confinement in fusion devices, and magnetic drug delivery in biomedical systems.

Studies in this area include the work of Ahmad et al. [?], who observed that mass flow increases with higher suction/injection parameters but decreases with an increase in the nonlinear Boussinesq approximation parameter. Similarly, Jha et al. [?] reported that an increase in suction/injection enhances the volume flow rate, whereas an increase in the Hartmann number leads to a reduction in flow rate. Yale and Musa [?] observed a reverse flow induced by suction, as evidenced by the concentration profile. Anyanwu and Raymond [?] found that increasing the Hartmann number results in a reduction in fluid velocity. Similarly, Ajibade et al. [?] reported that both fluid velocity and temperature decrease with enhanced suction. Usman et al. [?] noted that the heat transfer rate diminishes as the suction or injection parameters increase. Oni and Rilwanu [?] highlighted that fluid velocity rises when the Hartmann number decreases and drops as it increases. Ajibade and Bolaji [?] pointed out that an increase in the Hartmann number reduces skin friction on both plates, a finding also supported by Jha and Samaila [?] and Raju et al. [?], who likewise concluded that higher Hartmann numbers lead to reduced skin friction.

According to Amouzadeh et al. [?], the heat transfer rate rises with suction but falls with injection. Chitra and Suhasini [?] graphically demonstrated the influence of magnetic field parameters on velocity and temperature profiles under varying Hartmann numbers and suction/injection effects. Jha and Malgwi [?] observed that velocity distribution along the vertical main flow decreases with increasing Hartmann number in both symmetric and asymmetric wall heating conditions. Yao et al. [?] found that fluid velocity declines with higher suction values but increases with greater injection values. Chutia [?] also concluded that fluid velocity reduces as the Hartmann number increases. Palai et al. [?] reported that boundary layer thickness grows near the lower wall with injection, while it thins near the upper wall under suction. Chakradhar et al. [?] indicated that both suction and injection parameters rise with increasing volumetric flow rate and that pressure rise intensifies with higher Hartmann numbers. Hamrelaine et al. [?] concluded that an increase in the Hartmann number results in higher fluid velocity in both divergent and convergent channel configurations. Sarki et al. [?] found that the nonlinear convection parameter intensifies convective currents.

Similarly, Sajjan et al. [?] emphasized that the nonlinear Boussinesq approximation plays a significant role and cannot be neglected, as it strongly influences the flow behavior and heat transfer characteristics of the fluid. RamReddy et al. [?] examined the effects of the nonlinear Boussinesq approximation on natural convective flow. Srinivasacharya et al. [?] concluded that nonlinear convection parameters have a more pronounced impact on heat and mass transfer rates in Darcy porous media than in non-Darcy porous media. Wang et al. [?] observed that magnetic fields can induce a range of neurobiological effects. The combined effects of suction/injection, which modulate mass transport, and magnetic fields, which stabilize the flow, allow for precise manipulation of velocity and temperature profiles. This control is vital in practical applications including liquid-metal cooling in nuclear reactors, electromagnetic pumping, MHD power generation and metallurgical processes where maintaining flow stability, enhancing heat transfer and regulating boundary-layer development are key to maximizing efficiency, thermal performance and operational safety. Roshani et al. [?] concluded that a constant heat source leads to a wider spread of temperature distribution. Idowu and Olabode [?] reported that the fluid temperature increases with a rise in the heat-generation parameter, whereas the heat-absorption parameter reduces the temperature. In another article, Olabode et al. [?] observed that the velocity field increases with higher values of the nonlinear Boussinesq approximation parameter. Iranian et al. [?] demonstrated that an increase in the suction parameter leads to a reduction in the skin-friction profile. Daramola et al. [?] found that an increase in the suction/injection parameter enhances the skin-friction coefficient. Jha and Oni [?]

IJMSO

International Journal of Mathematical Sciences and Optimization: Theory and Applications
11(4), 2025, Pages 69 - 82
https://doi.org/10.5281/zenodo.18987204

showed that the nonlinear Boussinesq approximation contributes to an increase in fluid velocity, expansion of the reverse flow region near the walls. Isede et al. [?] analysed entropy optimization and heat transfer analysis of MHD heat generating fluid flow through an anisotropic porous parallel wall channel. Their findings show that magnetic field parameter reduce the dimensionless axial velocity. Nwaigwe et al. [?] observed that an increase in the suction parameter causes only a negligible change in the fluid temperature. Isede et al. [?] it was reported that the as the plate stretches, both the surface shear stress parameter and plate temperature exhibit higher values with injection compared to suction. Collectively, incorporating magnetohydrodynamics (MHD) broadens industrial applications ranging from electromagnetic casting and metallurgical processing to plasma confinement and biomedical drug delivery, where flow stability and heat transfer control are critical. Accounting for viscous dissipation and nonlinear buoyancy further enhances the realism of models for lubrication, polymer processing, and energy systems, thereby improving efficiency, durability, and safety. Collectively, these findings contribute to cost-effective design, optimized energy use, and greater operational reliability in thermo-fluid based industries.
Despite extensive research on natural convection Couette flow, the combined effects of suction/injection, magnetic fields and the nonlinear Boussinesq approximation in a vertical porous channel remain under explored. This study aims to address this gap by examining the influence of suction and injection on magnetohydrodynamic (MHD) natural convection Couette flow in such a channel, incorporating the nonlinear Boussinesq approximation, with particular emphasis on their effects on velocity, temperature, boundary-layer dynamics, and overall flow stability. By systematically analyzing the interplay of these factors, the study provides insights for optimizing heat transfer, controlling flow behavior, and enhancing boundary-layer management in practical engineering applications.

2 Mathematical Formulation

Consider a laminar flow of a viscous, incompressible and electrically conducting fluid subjected to magnetohydrodynamic (MHD) natural convection in the presence of suction/injection. Injection occurs at one wall $y = h$ while suction takes place at the opposite wall $y = 0$ to ensure mass conservation. The channel plate $y = 0$ is assumed to initiate motion with an impulsive velocity in the direction of flow development, as illustrated in Figure 1.

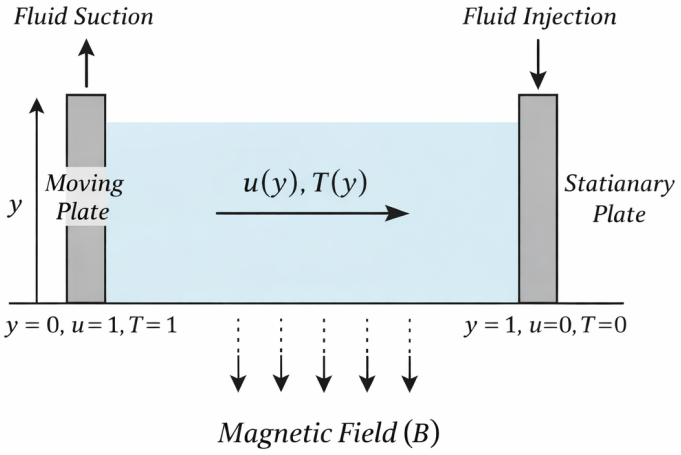

Figure 1: Diagrammatic representation of the problem

IJMSO
International Journal of Mathematical Sciences and Optimization: Theory and Applications
11(4), 2025, Pages 69 - 82
https://doi.org/10.5281/zenodo.18987204

The momentum and energy equations incorporating the nonlinear Boussinesq approximation are formulated as follows

$$\frac{d^2u}{dy^2} + SPr\frac{du}{dy} - M^2u + (1+\lambda T)T = 0, \tag{2.1}$$

$$\frac{d^2T}{dy^2} + SPr\frac{dT}{dy} = 0, \tag{2.2}$$

the dimensionless parameters employed in the above equations are defined as follows:

$$\begin{gathered} X = \frac{x}{b}, \quad Y = \frac{y}{b}, \quad T = \frac{T-T_0}{T_1-T_0}, \quad Pr = \frac{\nu}{\alpha}, \quad U_0 = \frac{\rho_0 g\beta(T_1-T_0)b^2}{\mu}, \\ U = \frac{u}{U_0}, \quad M^2 = \frac{\sigma B_0^2 b^2}{\rho\nu}, \quad S = \frac{V_0 b}{\nu}, \quad \lambda = \frac{\beta_1(T_1-T_0)}{\beta_0}, \end{gathered} \tag{2.3}$$

the corresponding boundary conditions are given as follows:

$$\begin{aligned} u = 1, \quad T = 1 \quad at \quad y = 0, \\ u = 0, \quad T = 0 \quad at \quad y = 1. \end{aligned} \tag{2.4}$$

The dimensionless forms corresponding to the boundary conditions are as follows:

$$y = \frac{y^*}{h}, \quad u = \frac{u^*}{U}, \quad T = \frac{T^*-T_0}{T_w-T_0}, \tag{2.5}$$

2.1 Homotopy Perturbation Method

By employing a convex homotopy, the momentum and energy equations (1) and (2) along with the boundary condition (4), are solved using the Homotopy Perturbation Method, as detailed below:

$$H(u,p) = (1-p)\left(\frac{d^2u}{dy^2}\right) + p\left(\frac{d^2u}{dy^2} + SPr\frac{du}{dy} - M^2u + (1+\lambda T)T\right) = 0, \tag{2.6}$$

$$H(T,p) = (1-p)\left(\frac{d^2T}{dy^2}\right) + p\left(\frac{d^2T}{dy^2} + SPr\frac{dT}{dy}\right) = 0. \tag{2.7}$$

Consequently, in the absence of an initial approximation, the equation takes the following form:

$$\frac{d^2u}{dy^2} = p\left(-S\frac{du}{dy} + M^2u - (1+\lambda T)T\right), \tag{2.8}$$

$$\frac{d^2T}{dy^2} = p\left(-SPr\frac{dT}{dy}\right). \tag{2.9}$$

The solutions to equations (1) and (2) are represented as follows:

$$u = u_0 + pu_1 + p^2u_2 + p^3u_3..., \tag{2.10}$$

$$T = T_0 + pT_1 + p^2T_2 + p^3T_3.... \tag{2.11}$$

By substituting equation (10) into equation (8) and equation (11) into equation (9), the following results are obtained:

$$\begin{aligned} \frac{d^2u_0}{dy^2} + p\frac{d^2u_1}{dy^2} + p^2\frac{d^2u_2}{dy^2} + ... = p\left(-S\frac{du_0}{dy} + M^2u_0 - T_0 - \lambda T_0^2\right) + p^2\left(-S\frac{du_1}{dy} + M^2u_1 - T_1 - 2\lambda T_0T_1\right) \\ + p^3\left(-S\frac{du_2}{dy} + M^2u_2 - T_2 - 2\lambda T_0T_2 - \lambda T_1^2\right) + ..., \end{aligned} \tag{2.12}$$

IJMSO
International Journal of Mathematical Sciences and Optimization: Theory and Applications
11(4), 2025, Pages 69 - 82
https://doi.org/10.5281/zenodo.18987204

$$\frac{d^2T_0}{dy^2} + p\frac{d^2T_1}{dy^2} + p^2\frac{d^2T_2}{dy^2} + ... = p\left(-SPr\frac{dT_0}{dy}\right) + p^2\left(-SPr\frac{dT_1}{dy}\right) + p^3\left(-SPr\frac{dT_2}{dy}\right) + ... \tag{2.13}$$

Equating the coefficients of the corresponding terms p^0, p^1, p^2 and p^3 in equations (12) and (13) gives:

$$p^0 : \frac{d^2u_0}{dy^2} = 0, \tag{2.14}$$

$$p^0 : \frac{d^2T_0}{dy^2} = 0, \tag{2.15}$$

$$p^1 : \frac{d^2u_1}{dy^2} = -S\frac{du_0}{dy} + M^2u_0 - (1+\lambda T_0)T_0, \tag{2.16}$$

$$p^1 : \frac{d^2T_1}{dy^2} = -SPr\frac{dT_0}{dy}, \tag{2.17}$$

$$p^2 : \frac{d^2u_2}{dy^2} = -S\frac{du_1}{dy} + M^2u_1 - (1+2\lambda T_0)T_1, \tag{2.18}$$

$$p^2 : \frac{d^2T_2}{dy^2} = -SPr\frac{dT_1}{dy}, \tag{2.19}$$

$$p^3 : \frac{d^2u_3}{dy^2} = -S\frac{du_2}{dy} + M^2u_2 - 2\lambda T_0T_2 - \lambda T_1^2, \tag{2.20}$$

$$p^3 : \frac{d^2T_3}{dy^2} = -SPr\frac{dT_2}{dy}. \tag{2.21}$$

$$\vdots$$

The boundary condition specified in equation (7) is rewritten as:

$$\begin{aligned} u_0(0) = 1, u_1(0) = u_2(0) = u_3(0) = ... = 0, \\ u_0(1) = u_1(1) = u_2(1) = u_3(1)... = 0, \\ T_0(0) = 1, T_1(0) = T_2(0) = T_3(0) = ... = 0, \\ T_0(1) = T_1(1) = T_2(1) = T_3(1)... = 0. \end{aligned} \tag{2.22}$$

Equations (23) and (24) are obtained by applying equations (14) and (15) along with the boundary conditions $u_0(0) = 1$ and $u_0(1) = 0$, $T_0(0) = 1$ and $T_0(1) = 0$, carrying out the required computations, as follows:

$$u_0 = A_1y + A_2, \tag{2.23}$$

$$T_0 = B_1y + B_2. \tag{2.24}$$

IJMSO

International Journal of Mathematical Sciences and Optimization: Theory and Applications
11(4), 2025, Pages 69 - 82
https://doi.org/10.5281/zenodo.18987204

Equations (25) and (26) are obtained by applying equations (16) and (17) along with the boundary conditions $u_1(0) = 0$ and $u_1(1) = 0$, $T_1(0) = 0$ and $T_1(1) = 0$ carrying out the required computations, as follows:

$$u_1 = \frac{Sy^2}{2} + M^2\left(\frac{y^2}{2} - \frac{y^3}{6}\right) - \left(\frac{y^2}{2} - \frac{y^3}{6}\right) - \lambda\left(\frac{y^2}{2} - \frac{y^3}{3} + \frac{y^4}{12}\right) + A_3y + A_4, \tag{2.25}$$

$$T_1 = \frac{SPry^2}{2} + B_3y + B_4. \tag{2.26}$$

Equations (27) and (28) are obtained by applying equations (18) and (19) along with the boundary conditions $u_2(0) = 0$ and $u_2(1) = 0$, $T_2(0) = 0$ and $T_2(1) = 0$ carrying out the required computations, as follows:

$$\begin{aligned} u_2 = &-\frac{S^2y^3}{6} - SM^2\left(\frac{y^3}{6} - \frac{y^4}{24}\right) + S\left(\frac{y^3}{6} - \frac{y^4}{24}\right) - \left(\frac{y^2}{2} - \frac{y^3}{6}\right) + S\lambda\left(\frac{y^3}{6} - \frac{y^4}{24} + \frac{y^5}{60}\right) \\ &- \frac{SA_3y^2}{2} + A_5y + A_6, \end{aligned} \tag{2.27}$$

$$T_2 = -\frac{S^2Pr^2y^3}{6} - \frac{SPrB_3y^2}{2} + B_5y + B_6. \tag{2.28}$$

Equations (29) and (30) are obtained by applying equations (20) and (21) along with the boundary conditions $u_3(0) = 0$ and $u_3(1) = 0$, $T_3(0) = 0$ and $T_3(1) = 0$ carrying out the required computations, as follows:

$$\begin{aligned} u_3 = &-\frac{S^3y^4}{24} + S^2M^2\left(\frac{y^4}{24} - \frac{y^5}{120}\right) - S^2\left(\frac{y^4}{24} - \frac{y^5}{120}\right) - \lambda S\left(\frac{y^4}{24} - \frac{y^5}{60} + \frac{y^6}{360}\right) + \frac{S^2A_3y^3}{6} \\ &- \frac{SA_5y^2}{2} - \frac{M^2S^2y^5}{120} - SM^4\left(\frac{y^5}{120} - \frac{y^6}{720}\right) + \lambda SM^2\left(\frac{y^5}{120} - \frac{y^6}{720} + \frac{y^7}{2520}\right) + \frac{A_5M^2y^3}{6} \\ &- \frac{SM^2A_3y^4}{24} + SM^2\left(\frac{y^5}{120} - \frac{y^6}{720}\right) + \frac{S^2Pr^2y^5}{120} + \frac{SPrB_3y^5}{24} - \frac{B_5y^3}{6} + \frac{\lambda SPrB_3y^4}{12} \\ &- \lambda B_5y^2 - \frac{\lambda S^2Pr^2y^6}{90} - \frac{\lambda SPrB_3y^5}{20} + \frac{\lambda B_5y^3}{3} - \frac{\lambda S^2Pr^2y^6}{120} - \frac{\lambda SPrB_3y^4}{12} - \lambda B_3^2y^2 \\ &+ A_7y + A_8, \end{aligned} \tag{2.29}$$

$$T_3 = \frac{S^3Pr^3y^4}{24} + \frac{S^2Pr^2B_3y^3}{6} - SPrB_5y^2 + B_7y + B_8. \tag{2.30}$$

where,

$$A_1 = B_1 = -1, \quad A_2 = B_2 = 1, \quad A_3 = \frac{-S}{2} - \frac{M^2}{3} + \frac{1}{3} + \frac{\lambda}{4}, \quad A_4 = 0, \quad B_3 = \frac{-SPr}{2}, \quad B_4 = 0,$$

$$A_5 = \frac{S^2}{6} + \frac{SM^2}{8} - \frac{S}{8} - \frac{\lambda S}{10} + \frac{SA_3}{2}, \quad B_5 = \frac{S^2Pr^2}{6} + \frac{SPr}{2},$$

$$\begin{aligned} A_7 = &-\frac{S^3}{24} - \frac{13S^2M^2}{40} + \frac{S^2}{30} + \frac{\lambda S^2}{36} - \frac{S^2A_3}{6} + \frac{SA_5}{2} + \frac{SM^4}{144} - \frac{SM^2}{144} - \frac{\lambda SM^2}{168} + \frac{SM^2A_3}{24} \\ &- \frac{M^2A_5}{6} - \frac{S^2Pr^2}{120} - \frac{SPrB_3}{24} + \frac{B_5}{6} + \frac{2\lambda B_5}{3} + \frac{\lambda SPrB_3}{20} + \frac{\lambda S^2Pr^2}{360} + \lambda B_3^2, \end{aligned}$$

IJMSO

International Journal of Mathematical Sciences and Optimization: Theory and Applications
11(4), 2025, Pages 69 - 82
https://doi.org/10.5281/zenodo.18987204

$$B_7 = \frac{SPrB_5}{2} - \frac{S^2Pr^2B_3}{6} - \frac{S^3Pr^3}{2}, \quad A_6 = B_6 = A_8 = B_8 = 0.$$

Equations (23) - (30) provide the approximate expressions for velocity and temperature as follows:

$$u = u_0 + u_1 + u_2 + ..., \tag{2.31}$$

$$T = T_0 + T_1 + T_2 + ... \tag{2.32}$$

The skin friction at the channel's fluid boundary surfaces is obtained by differentiating Equation (31) with respect to y and then evaluating it at the boundaries $y = 0$ and $y = 1$ as follows:

$$\tau_0 = -1 + A_3 + A_5 + A_7, \tag{2.33}$$

$$\tau_1 = -\frac{3}{2} + S\left(\frac{4}{3} - \frac{S}{2} - \frac{M^3}{3} + \frac{\lambda}{3}\right) + \frac{M^2}{2} - \frac{\lambda}{2} + A_3(1-S) + A_5 + A_7. \tag{2.34}$$

The expression for the mass flux is derived as: $Q_m = \int_0^1 u(y)dy$, we derived as:

$$\begin{aligned} Q_m = {} & \frac{3}{8} + \frac{S}{5} + \frac{M^2}{8} - \frac{\lambda}{10} + \frac{A_3}{2} - \frac{7S^2}{144} - \frac{17SM^2}{720} + \frac{\lambda S}{36} - \frac{SA_3}{6} + \frac{A_5}{2} + \frac{S^3}{120} + \frac{S^2M^2}{180} - \frac{S^2A_3}{24} \\ & - \frac{SA_5}{6} - \frac{SM^4}{144} - \frac{\lambda B_5}{4} - \frac{\lambda SPrB_3}{120} - \frac{\lambda S^2Pr}{5040} + \frac{\lambda SM^2}{168} - \frac{SM^2A_3}{24} + \frac{S^2Pr^2}{720} + \frac{SPrB_3}{60} \\ & - \frac{B_5}{24} - \frac{\lambda B_3^2}{2} + \frac{A_7}{2}. \end{aligned} \tag{2.35}$$

3 Results and Discussion

The effects of natural convection Couette flow under the influence of suction/injection and the nonlinear Boussinesq approximation were investigated. Additionally, a MATLAB program was developed to generate line graphs illustrating the velocity and temperature profiles, thereby enhancing the understanding of the problem. The study explores the impact of physical parameters such as the Prandtl number, suction/injection, nonlinear Boussinesq approximation and Hartmann number. Figures 2 and 3 illustrate the effect of suction/injection on fluid velocity and temperature when $Pr = 0.71$, $\lambda = 6.0$ and $M = 0.6$. It is important to note that a negative values of indicates suction at the heated plate with a corresponding injection at the cold plate. Under these conditions, an increase in suction at the heated plate results in a reduction in the channel temperature as shown in Figure 2. This outcome is physically expected, as the horizontal fluid motion opposes the heat flux from the heated plate. The drop in temperature weakens the convection currents, leading to a decrease in fluid velocity. Conversely, when fluid is injected through the heated plate, the enhanced horizontal flow and heat transfer increase the fluid temperature within the channel. As a result, both temperature and velocity rise with increasing injection. Suction helps reduce fluid temperatures and prevent overheating, while injection enhances heat transfer and fluid mixing, benefiting systems like heat exchangers, chemical reactors and microfluidic devices.

Figures 4 and 5 present the temperature and velocity profiles for various values of the Prandtl number and . As shown in Figure 4, fluid temperature decreases with increasing Prandtl number, a trend that is expected, since higher Prandtl numbers correspond to lower thermal diffusivity. This reduction in thermal diffusivity lowers the fluid temperature. Consequently, the resulting stronger convection currents lead to an increase in fluid velocity as depicted in Figure 5. In addition, higher Prandtl number fluids, with lower thermal diffusivity, enhance convective heat transfer and fluid velocity, making them useful for efficient cooling and controlled flow in engineering and industrial systems.

IJMSO

International Journal of Mathematical Sciences and Optimization: Theory and Applications
11(4), 2025, Pages 69 - 82
https://doi.org/10.5281/zenodo.18987204

Figure 6 depicts the impact of the Hartmann number on the velocity profile of the fluid. An increase in the Hartmann number leads to a marked decrease in fluid velocity, underscoring the magnetic fields pivotal role in regulating magnetohydrodynamic (MHD) flow. This overall reduction in velocity is primarily due to the strengthening of the Lorentz force, which acts in opposition to the fluid motion. As the Hartmann number rises, the magnetic damping effect intensifies, which is a well-established characteristic of MHD behavior. In addition, as the Hartmann number increases, the Lorentz force becomes more pronounced, acting as a resistive force against fluid motion and causing a notable decrease in velocity. The magnetic damping effect plays a critical role in enhancing flow stabilization and promoting boundary-layer formation, serving as a fundamental mechanism for the regulation of magnetohydrodynamic (MHD) flows. Variation in the Hartmann number allows magnetic fields to modulate fluid velocity, stabilize the flow, and shape boundary layers, with significant practical applications in liquid-metal cooling systems, electromagnetic pumps, MHD generators, and metallurgical processes.
Figure 7 presents the influence of the nonlinear Boussinesq approximation on the velocity profile. As the strength of the nonlinear Boussinesq approximation increases, two contrasting velocity trends emerge within the channel. Near the heated plate, an increase in velocity is observed, while near the cold plate, a corresponding decrease in velocity occurs. Moreover, increasing the strength of the nonlinear Boussinesq approximation heightens the responsiveness of buoyancy forces to velocity variations, thereby enhancing convective motion near the heated wall while suppressing it near the cooler wall. This leads to asymmetrical velocity distributions and may give rise to more intricate flow dynamics. Furthermore, the nonlinear Boussinesq approximation significantly influences velocity distributions, and controlling these effects can optimize heat transfer and flow in industrial systems such as heat exchangers, electromagnetic pumps, nuclear reactor cooling, and metallurgical processes, enhancing efficiency and safety.

Table 1 presents the numerical values of skin friction. It is evident that skin friction on both the moving and stationary plates increases with higher injection rates. An increase in injection rate leads to stronger momentum exchange near the walls, which elevates the velocity gradient and, consequently, the skin friction on both the moving and stationary plates. Physically, this reflects greater wall shear stress and resistance to fluid motion, a direct outcome of the enhanced mass and momentum being introduced into the boundary layer. The table indicates that an increase in the nonlinear Boussinesq approximation and the Hartmann number also leads to a rise in skin friction on both plates. Finally, Nonlinear Boussinesq approximation amplifies temperature driven buoyancy, steepening velocity gradients at the walls and raising skin friction and higher Hartmann numbers increase magnetic damping, requiring stronger wall gradients to sustain flow, which also elevates skin friction.

Table 2 presents the computed mass flux values, showing that mass flux diminishes with increasing injection rates. An increase in the injection rate introduces additional fluid near the wall, which disrupts the axial flow structure by thickening the boundary layer and reducing the streamwise velocity. This disturbance can lead to a reduction in the overall mass flux through the channel, particularly in wall-driven flows such as Couette flow, where near-wall conditions significantly influence the flow dynamics.

4 Conclusion

An analytical investigation has been conducted on natural convection Couette flow of an electrically conducting fluid in a vertical porous channel, focusing on the effects of a nonlinear Boussinesq approximation parameter. The governing momentum and energy equations formulated to represent the physical system, are solved using the Homotopy Perturbation Method (HPM). The key findings of the study are summarized as follows:
• an increase in the Hartmann number substantially suppresses fluid velocity,

IJMSO
International Journal of Mathematical Sciences and Optimization: Theory and Applications
11(4), 2025, Pages 69 - 82
https://doi.org/10.5281/zenodo.18987204

• an increase in suction at the heated plate leads to a decrease in the temperature within the channel,
• fluid temperature diminishes as the Prandtl number increases,
• the presence of a nonlinear Boussinesq approximation causes a notable increase in velocity,
• an increase in the nonlinear Boussinesq approximation parameter and Hartmann number leads to higher skin friction on both the moving and stationary plates.

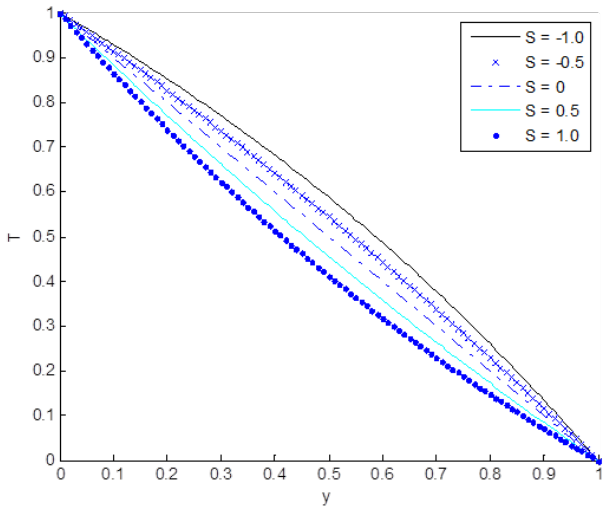

Figure 2: Temperature profile for different values of $S(Pr = 0.71, \lambda = 6.0, M = 0.6)$

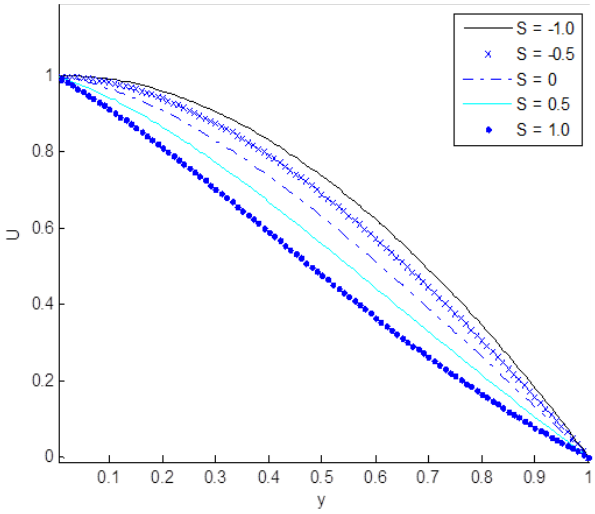

Figure 3: Velocity profile for different values of $S(Pr = 0.71, \lambda = 6.0, M = 0.6)$

IJMSO

International Journal of Mathematical Sciences and Optimization: Theory and Applications
11(4), 2025, Pages 69 - 82
https://doi.org/10.5281/zenodo.18987204

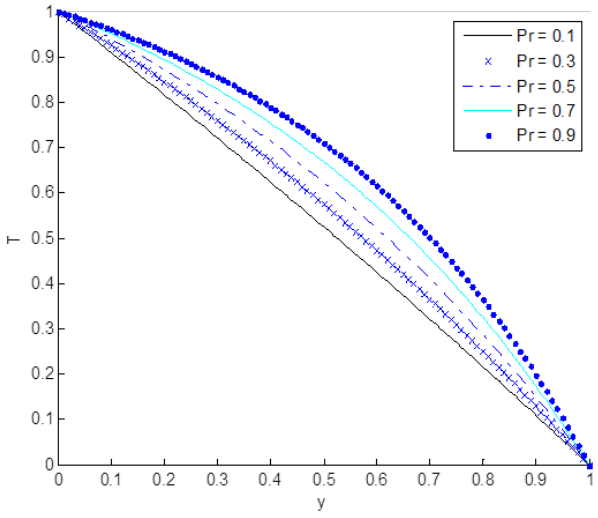

Figure 4: Temperature profile for different values of $Pr(S = -1.0, \lambda = 6.0, M = 0.6)$

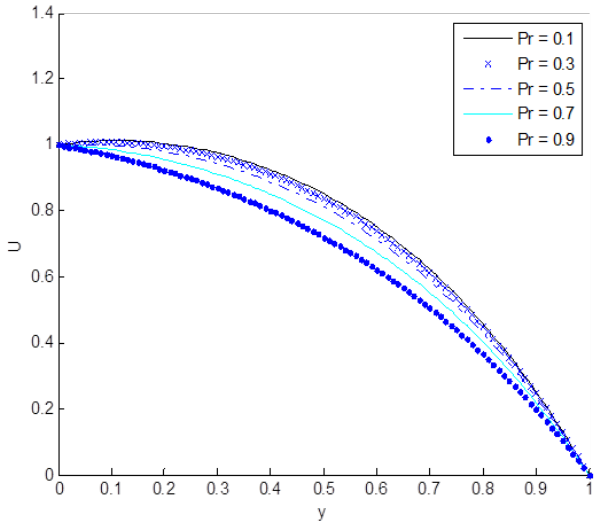

Figure 5: Velocity profile for different values of $Pr(S = -1.0, \lambda = 6.0, M = 0.6)$

IJMSO

International Journal of Mathematical Sciences and Optimization: Theory and Applications
11(4), 2025, Pages 69 - 82
https://doi.org/10.5281/zenodo.18987204

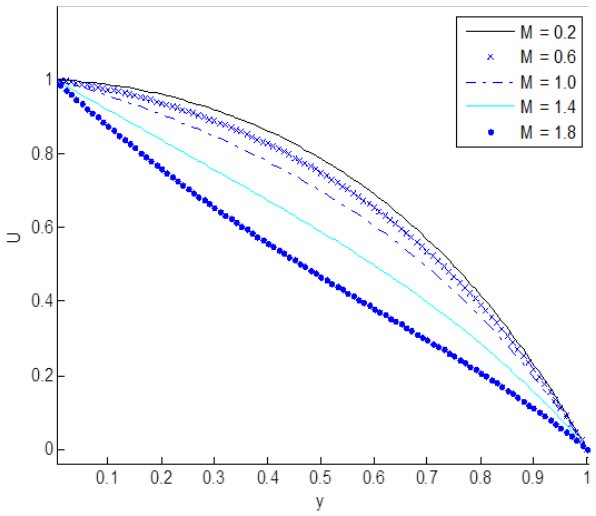

Figure 6: Velocity profile for different values of $M(Pr = 0.71, S = -1.0, \lambda = 6.0)$

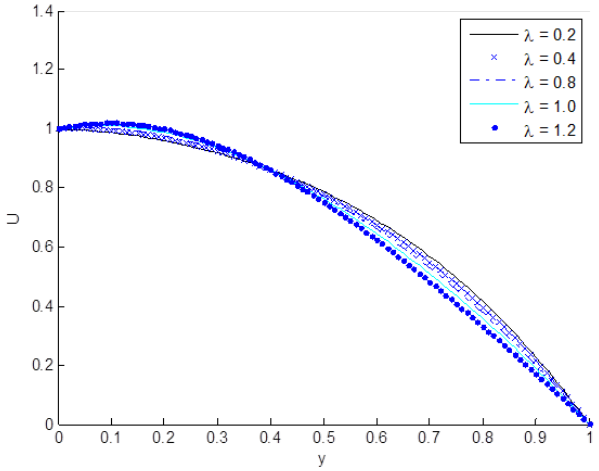

Figure 7: Velocity profile for different values of $\lambda(Pr = 0.71, S = -1.0, M = 0.6)$

IJMSO

International Journal of Mathematical Sciences and Optimization: Theory and Applications
11(4), 2025, Pages 69 - 82
https://doi.org/10.5281/zenodo.18987204

Table 1: Skin friction at the plate $y = 0$ and $y = 1$

	$\lambda = 0.5, M = 1.0$		$\lambda = 0.5, M = 2.0$		$\lambda = 1.0, M = 2.0$	
S	τ_0	τ_1	τ_0	τ_1	τ_0	τ_1
0.5	1.1287	0.7745	2.1889	1.0014	3.8132	1.9382
1.0	1.4023	1.1939	2.5185	2.1435	4.1973	2.4473
1.5	1.6959	1.6334	2.8640	3.3015	4.5689	3.9439
2.0	2.0094	2.0928	3.2252	4.4752	4.9280	4.5698
2.5	2.3439	2.5721	3.6022	5.6647	5.2745	6.8995

Table 2: Estimated numerical values of mass flux Q

	$\lambda = 0.5, M = 1.0$	$\lambda = 0.5, M = 2.0$	$\lambda = 1.0, M = 2.0$
S	Q	Q	Q
0.5	0.4710	0.3352	0.0643
1.0	0.4297	0.2904	0.0453
1.5	0.3896	0.2541	0.1361
2.0	0.3518	0.2274	0.2070
2.5	0.3173	0.2113	0.2002

References

[1] Ahmad, S. K., Jha, B. K., Hussaini, A. M., and Altine, M. M. (2022). MHD free-convective Couette flow in a vertical porous microchannel using non-linear Boussinesq approximation. Journal of Applied Sciences, Information and Computing. 3(2), 25 - 34.

[2] Jha, B. K., Aina, B., and Ajiya, A. T. (2015). Role of suction/injection on MHD natural convection flow in a vertical microchannel. International Journal of Energy and Technology. 7(2), 30 - 39.

[3] Yale, I. D., and Musa, M. (2022). Unsteady MHD Couette flow in a vertical porous channel with effect of thermal radiation and variable temperature. Global Journal of Engineering and Technology Advances. 10(3), 85 - 94. https://doi.org/10.30574/gjeta.2022.10.3.00270 .

[4] Anyanwu, E. O., and Raymond, D. (2023). Effects of Hartmann number on unsteady MHD flow in a porous medium bounded by parallel plate. Asian Journal of Pure and Applied Mathematics. 5(1), 396 - 41.

[5] Ajibade, A. O., Umar, A. M., and Tafida, M. K. (2021). An analytical study on effect of viscous dissipation and suction/injection on a steady MHD natural convection Couette flow of heat generating/absorbing fluid. Advances in Mechanical Engineering. 13(5), 1 - 12.

[6] Usman, H., Dogondaji, A. M. and Sammani, A. (2023). Effect of suction/injection on unsteady MHD natural convective radiative flow of heat mass transfer in a plumb frequency. Saudi Journal of Engineering and Technology. 8(7), 171 - 180.

[7] Oni, M. O., and Rilwanu, U. (2023). Role of suction/injection on electromagnetohydrodynamic natural convection flow in a porous microchannel with electro osmotic effect. International Journal of Applied Mechanics and Engineering. 28(4), 94 - 113.

[8] Ajibade, A. O., and Bolaji, S. (2020). Steady natural convection MHD flow in a vertical channel with induced magnetics field and variable fluid properties. Journal of Mathematical Science Series. 47(1), 176 - 192.

[9] Jha, B. K. and Samaila, G. (2022). Nonlinear approach for natural convection and mass transfer in a vertical channel. doi:10.1002/htj.223443.

[10] Raju, S. R., Reddy, G. J., Rao, J. A., and Rashidi, M. M. (2016). Thermo diffusion and diffusion thermo effects on an unsteady heat and mass transfer MHD natural convection Couette flow using FEM. Journal of Computational Design and Engineering. 3, 349 - 362.

[11] Amouzadeh, F., Tondro, M., Asadi, Z., and Ganji, D. D. (2021). Suction and injection effect on MHD fluid flow within a vertical annulus for electrical wire cooling. Case Studies in Thermal Engineering. 27; 101241. https://doi.org/10.1016/j.csite.2021.101241.

[12] Chitra, M., and Suhasini, M. (2017). Effect of suction/injection on unsteady MHD oscillatory flow through a vertical channel filled with porous medium. Research Journal of Science and Technology. 9(4), 498 - 504.

[13] Jha, B. K., and Malgwi, P. B. (2022). Hydromagnetic free convection flow in a vertical microporous channel with hall current and ion slip effect. Journal of the Egyptian Mathematical Society. 30(21), 2 - 26. https://doi.org/10.1186/s42787-022-00155-w.

[14] Yao, S. W. Ahmad, M. Mustafa, I., Ahmad, I., Asjad, M. I., and Nazar, M. (2022). Suction effect on MHD flow of Brinkman-type fluid with heat absorption and first-order chemical reaction. frontiers in energy research. 10:963583, doi: 10.3389/fenrg.2022.963583.

[15] Chutia, M. (2022). Numerical solution of MHD channel flow in a porous medium with uniform suction and injection in the presence of an inclined magnetic field. Journal of Applied Mathematics and Computational Mechanics. 21(2), 5 - 13. dOI: 10.17512/jamcm.2022.2.01.

[16] Palai, D. P., Chaudhuri, S., and Das, B. (2025). Effects of uniform injection and suction on the flow of a rivlin-ericksen fluid of grade three through porous parallel plates: A semi-analytical study. Journal of Heat and Mass Transfer Research. 12(1), 45 - 60. https://doi.org/10.22075/JHMTR.2024.32255.1496.

[17] Chakradhar, K. Nandagopal, K. Prashanthi, V. Parandhama, A. Somaiah. T. Thrinath, B. V., Tarakaramu, N., Rasool, G., and Abduvalieva, D. (2025). MHD effect on peristaltic motion of williamson fluid via porous channel with suction and injection. Partial Differential Equations in Applied Mathematics. 13, 101103.

[18] Hamrelaine, S., Mebarek-Oudina, F., and Sari, M. R. (2019). Analysis of MHD jeffery hamel flow with suction/injection by homotopy analysis method. Journal of Advanced Research in Fluid Mechanics and Thermal Sciences. 58(2), 173 - 186.

[19] Sarki, M. N., Hamza, M. S., and Tanko, A. (2025). Impact of chemical reaction, soret effects on nonlinear free convection mass transfer in Couette flow within a vertical channel. International Journal of Innovative Mathematics, Statistics and Energy Policies. 13(2), 100 - 113 .

[20] Sajjan, K., Shah, N. A., Ahammad, N. A., Raju, C. S. K., Kumar, M. D., and Weera, W. (2022). Nonlinear Boussinesq and Rosseland approximations on 3D flow in an interruption of ternary nanoparticles with various shapes of densities and conductivity properties. AIMS Mathematics. 7(10), 18416 - 18449. dOI: 10.3934/math.20221014.

[21] RamReddy, C., Naveen, P., and Srinivasacharya, D. (2019). Influence of nonlinear Boussinesq approximation on natural convective flow of a power-law fluid along an inclined plate under convective thermal boundary condition. Nonlinear Engineering. 8, 94 - 106.

[22] Srinivasacharya, D., RamReddy, C., and Naveen, P. (2018). Effects of nonlinear Boussinesq approximation and double dispersion on a micropolar fluid flow under convective thermal condition. Heat Transfer. 48(1), 414 - 434. https://doi.org/10.1002/htj.21391.

[23] Wang, X., Ye, Y., Zuo, H., and Li, Y. (2024). Neurobiological effects and mechanisms of magnetic fields: a review from 2000 to 2023. BMC Public Health. 24:3094. https://doi.org/10.1186/s12889-024-18987-9.

[24] Roshani, H., Jalili, P., Jalili, B., and Ganji, D. D. (2024). Impact of various heat sources on the transient heat transfer rate in a 3D cylinder consisting of parts with different thermal conductivity coefficients. International Journal of Thermofluids. 23, 100799.

[25] Idowu, A. S., and Olabode, J. O. (2021). Dynamics of heat generating upper-convected maxwell fluid in a porous medium over melting stretching sheet with stratification. Journal of Applied Sciences, Information and Computing. 2(1), 12 - 23.

[26] Olabode, J. O., Idowu, A. S., Akolade, M. T., and Titiloye, E. O. (2021). Unsteady flow analysis of Maxwell fluid with temperature dependent variable properties and quadratic thermo-solutal convection influence. Partial Differential Equations in Applied Mathematics. 4, 100078.

[27] Iranian, D. Sudarmozhi, K., Khan, I., and Mohamed, A. (2023). Significance of heat generation and impact of suction/injection on Maxwell fluid over a horizontal plate by the influence of radiation. International Journal of Thermofluids. 20, 100396.

[28] Daramola, D. A., Ajibade, A. O., and Lawal, H. A. (2023). Role of suction/injection on mixed convection flow in a vertical microchannel filled with porous material. FUDMA Journal of Sciences. 7(3), 293 - 303.

[29] Jha, B. K., and Oni, M. (2020). Nonlinear mixed convection flow in an inclined channel with time-periodic boundary condition. International Journal of Engineering Physics. 6, 21 - 33.

[30] Isede, H. A., Adeniyan, A., and Oladosu, O. O. (2023). Entropy optimization and heat transfer analysis of MHD heat generating fluid flow through an anisotropic porous parallel wall channel: An analytic solution. International Journal of Mathematical Sciences and Optimization: Theory and Applications. 9(1), 81 - 103.

[31] Nwaigwe, C., Weli, A., and Mebarek-Oudina, F. (2023). Modelling the impacts of shape and volume fraction of nanoparticles on water based nanofluid flow with variable thermophysical properties. International Journal of Mathematical Sciences and Optimization: Theory and Applications. 8(2), 94 - 108.

[32] Isede, H. A., Adeniyan, A., and Ogbonna, N. (2023). Lie-group analysis of flow and heat transfer of a dissipating fluid past stretching/shrinking surfaces with variable viscosity and non-uniform heat flux. International Journal of Mathematical Sciences and Optimization: Theory and Applications. 9(1), 59 - 80.